Scale-free network with Boolean dynamics as a function of connectivity

A. Castro e Silva,[1,*] J. Kamphorst Leal da Silva,[1,†] and J. F. F. Mendes[2,‡]
[1]*Departamento de Física, Universidade Federal de Minas Gerais, Caixa Postal 702, 30.123-970 Belo Horizonte/MG, Brazil*
[2]*Departamento de Física, Universidade de Aveiro, Campus Universitário de Santiago, 3810-193 Aveiro, Portugal*
(Received 14 June 2004; revised manuscript received 7 September 2004; published 28 December 2004)

In this work we analyze scale-free networks with different power-law spectra $N(k) \sim k^{-\gamma}$ under a Boolean dynamic, where the Boolean rule that each node obeys is a function of its connectivity k. This is done by using only two logical functions (AND and XOR) which are controlled by a parameter q. Using a damage spreading technique we show that the Hamming distance and the number of 1's exhibit power-law behavior as a function of q. The exponents appearing in the power laws depend on the value of γ.

DOI: 10.1103/PhysRevE.70.066140 PACS number(s): 05.10.−a, 05.45.−a, 87.18.Sn

I. INTRODUCTION

This paper blends two promising concepts of complex systems: namely, the Boolean networks [1,2] and models of growing networks [3,4]. The former was introduced by Kauffman [1,2] in 1969. One important thing about Kauffman's model is that it was very well received not just by the physical but by the biological community as well. The simplicity and richness of the behaviors of this model created a huge field of research, with many types of different Boolean networks [5]. Moreover, this model became a good candidate to explain biological problems such as cell differentiation, gene expression, protein interaction, and genetic regulatory networks [6–8]. A Boolean network is a complex dynamical system constituted of logical variables connected by logical functions. The simplest Boolean model has two parameters: the number of logical variables, N, and the number of inputs of their Boolean functions, K, where K varies from $K=1$ (the function has just one input) to $K=N$ (all variables connected with all the others including itself). The Boolean functions are chosen randomly in the beginning, and they are kept during the dynamics. The network updates synchronously, meaning that all nodes refresh their state at the same time. This kind of network exhibits an ordered dynamic for $K=1$ and a chaotic one when $K=N$. However, the network self-organizes, showing an interesting level of order and complexity at $K=2$, the edge of chaos. In addition to Darwin's natural selection and random mutation, Kauffman's idea is that self-organization and random dynamic can be responsible for the complexity observed in nature.

The models of growing networks introduced by Barabási and Albert [3,4] are on the other side. In these works was proposed a very elegant way of creating a self-organized scale-free structure. In contrast to most types of networks previously known, the scale-free ones exhibit a power-law distribution of connections, $P(k) \sim k^{-\gamma}$, where γ is the so-called scale-free exponent [9]. This behavior is similar to what happens with lengths in fractal structures. The mechanism that makes possible the arising of such a property is the so-called *preferential attachment*; that is, the probability of an old node to receive a new link from a new node is proportional to the number of preexistent connections in this node. The growing nature of these networks allows the study of a wide type of networks, such as the World Wide Web, neural, social relations, disease spreading, voting, citations of scientific papers, movie's actors interconnections, etc. [10–21]. The second characteristic of a scale-free network is the *small world effect*, which means that the shortest distance between two nodes is of the order of $\ln(N)$, where N is the size of the network. In other words, no matter how large the network could be, any two nodes are connected via a relatively small chain of links. For instance in WWW any document can be reached with fewer than 19 mouse clicks. The third feature of scale-free graphs is the very good tolerance to random removal of a significant fraction of its nodes conjugated with a high vulnerability to directional attacks to the most connected nodes (hubs).

Although these two branches of research are expanding, with a huge amount of publications, the combination of both is just in the beginning, and little is known about the behavior of random networks under scale-free topology.

Since scale-free networks describe more realistically interactions among members of any types of network, the Boolean dynamic can help to understand how some sort of dynamics flows inside those groups with that topology. From the biologic point of view, the introduction of the scale-free structure can be a decisive step to describe in a qualitative and quantitative fashion what is observed in genetic networks, metabolic pathways, and protein interaction networks [28]. All these networks have developed from very simple ones under the pressure of natural selection. They have evolved by gradual changes (mutations) that, simultaneously, keep its functionality. Therefore we expect that scale-free networks are a more realistic description since they are growing graphs. It is worth mentioning that scale-free networks are more robust to random errors than homogeneous random models. Experimental evidence has been found in cellular networks of some living beings—for example, the yeast *Saccharomyces cerevisiae* [23].

Few papers have been published using Boolean dynamics in scale-free networks. Fox and Hill used a random dynamics

*Electronic address: alcides@fisica.ufmg.br
†Electronic address: jaff@fisica.ufmg.br
‡Electronic address: jfmendes@fis.ua.pt

in a network with maximum connectivity $K_{max}=30$ to simulate the regulation of gene expression [22]. Aldana and Cluzel analytically demonstrated the existence of a phase transition for values of the scale-free exponent in the open interval (2, 2.5) in the random dynamics [24].

In this work we study scale-free networks with a deterministic Boolean dynamics using numerical simulations. We consider that the dynamics is driven only by AND and XOR functions. These functions are controlled by an external parameter q. This simple dynamics allows us to simulate large networks. We consider the Hamming distance D [27] and the number of 1's, M, for asymptotic times and different values of q. After averaging for several initial conditions we find that these quantities vary with q as power laws.

In the following section we define the scale-free networks and the Boolean dynamics. Section III presents our results for the numerical simulations, which are then discussed in Sec. IV. A brief summary is given in Sec. V.

II. NETWORKS AND THE DYNAMICS

The computer simulation was performed in two major parts. The first part was the growth of the network, which corresponds to the static part of the simulation since the network is unchangeable during the dynamics. We grew scale-free networks with minimum connectivity $k_{min}=1$ and $k_{min}=2$ by using the *growing network with redirection* algorithm [25]. The minimum connectivity corresponds to the smallest number of links that a node can have. The two kinds of network are grown as follows.

(i) $k_{min}=1$. A new node is linked to only one old node; we select an old node with uniform probability, and then the link with the old node is established with probability $1-r$ or it is redirected to the ancestor of the old node with probability r.

(ii) $k_{min}=2$. A new node is linked to two old nodes; we select an old node with uniform probability, and then one link with the old node is established with probability $1-r$ or it is redirected to one of the two ancestors of that node with probability r. We repeat the same procedure for the other link.

In both cases, the initial condition consists of three nodes with cyclic connections. This algorithm creates a scale-free network with $\gamma=r^{-1}+1$. For instance, when $r=0.5$, the network has $\gamma=3$, corresponding to a growth with linear preferential attachment. We use different values of r for the two kinds of networks.

The second part of the simulation is the dynamic itself. Once the network is made of N nodes connected by links, to each node i is assigned a logical variable $\sigma_i(t)$. The state of the network at time t is represented by a set of Boolean variables $\mathbf{(}\sigma_1(t),\sigma_2(t),\sigma_3(t),\ldots,\sigma_N(t)\mathbf{)}$. At each time step, the state of a node i is defined in the following way.

(i) For $k_{min}=2$, $\sigma_i(t+1)$ is given by $F_i\mathbf{(}\sigma_{i_1}(t),\sigma_{i_2}(t),\ldots,\sigma_{i_{k_i}}(t)\mathbf{)}$. In other words, the state of a node i at $t+1$ is a function of the states at t of all nodes linked with i—namely, $\sigma_{i_1}(t),\sigma_{i_2}(t),\ldots,\sigma_{i_{k_i}}(t)$, where k_i is the connectivity of the ith node.

(ii) For $k_{min}=1$, the state of a node is defined in a different way, since there are nodes with just one link. Then $\sigma_i(t+1)$ is given by $F_i\mathbf{(}\sigma_i(t),\sigma_{i_1}(t),\sigma_{i_2}(t),\ldots,\sigma_{i_{k_i}}(t)\mathbf{)}$. Now, the state of a node i at $t+1$ is a function of the state at t of all nodes linked to it and of its own state as well. In this way we have always a function with at least two inputs.

Finally we define the function $F_i(\sigma)$:

$$F_i=\begin{cases}\text{AND} & \text{if } k_i<q,\\ \text{XOR} & \text{otherwise},\end{cases} \tag{1}$$

where q is a threshold parameter that controls how the logical functions AND and XOR spread into the network. The AND and XOR logical functions were introduced in order to simplify the model, avoiding the necessity of defining 2^{2^k} different Boolean relations for each node. It is know from previous works that the AND function leads to an ordered regime (with two fixed points, where all variables are 0's or 1's) while the XOR introduces a more chaotic component to the dynamic. These kinds of functions are necessary to study biologic networks since they are the Boolean counterparts of real reactions in cell regulatory system [2,7]. Once in the scale-free network, we have many nodes poorly connected (small k) and few nodes highly connected (large k), Eq. (1). We can set a balance between chaotic and ordered dynamics inside the network.

An initial state $\Sigma=\mathbf{(}\sigma_1(0),\sigma_2(0),\sigma_3(0),\ldots,\sigma_N(0)\mathbf{)}$ is created by assigning randomly 0's and 1's to all nodes. A copy $\overline{\Sigma}=\mathbf{(}\overline{\sigma_1}(0),\overline{\sigma_2}(0),\overline{\sigma_3}(0),\ldots,\overline{\sigma_N}(0)\mathbf{)}$ of the initial state is also created, and we introduce a damage by changing the value of one randomly chosen node. Both the initial state and the damaged state evolve under the control of Eq. (1). Once the new state of all nodes is calculated, the entire network is updated (synchronous update) and the system goes to the next Monte Carlo time step (MCS). Note that, except for the random choice of the initial state, the dynamics is deterministic. This means that the Boolean functions act with a probability $p=1$, and this is another simplification to the dynamics. Random variables are important in order to simulate real genetic networks under influence of many uncertainties like biologic variability, experimental noise, and interacting variables impossible to quantify. However, this simplification allows us to consider large networks without loss of complexity in the dynamical behavior.

III. SIMULATION DATA AND RESULTS

The dynamical behavior is characterized by two quantities. The first is the average density of 1's—namely,

$$M(q,t)=\lim_{N\to\infty}\left\langle\frac{1}{N}\sum_{i=1}^{N}\sigma_i(t)\right\rangle. \tag{2}$$

The second is the average of the Hamming distance, which is defined by

$$D(q,t)=\lim_{N\to\infty}\left\langle\frac{1}{N}\sum_{i=1}^{N}|\sigma_i(t)-\overline{\sigma_i(t)}|\right\rangle. \tag{3}$$

Here, $\langle\cdots\rangle$ is the average for different initial conditions. An initial condition is given not only by the initial states

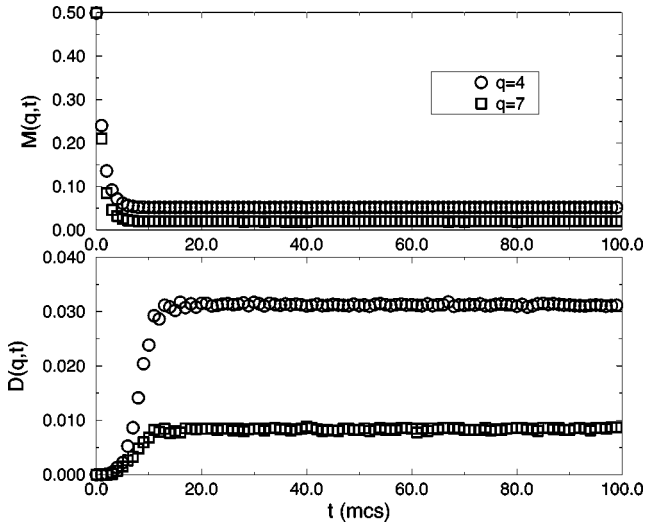

FIG. 1. Plots of $M(q,t)$ vs t and $D(q,t)$ vs t for a network with $N=8\times10^4$, $k_{min}=1$, and $r=0.5$.

$(\Sigma,\overline{\Sigma})$ but also by one set of links of a grown network with a specific γ.

After a very short transient (less than 30 time steps) these quantities reach the stationary values $M(q)$ and $D(q)$, as is shown in Fig. 1 for a network with $N=8\times10^4$ nodes, $k_{min}=1$, and $r=0.5$. The stationary values, defined as

$$M(q)=\lim_{T\to\infty}1/T\int_t^{t+T}M(q,t')dt',$$

$$D(q)=\lim_{T\to\infty}1/T\int_t^{t+T}D(q,t')dt',$$

were determined by discarding the first 50 time steps and by making a time average until $t=200$ time steps. We can also see in the figure that the stationary values $D(q)$ and $M(q)$ depend on q. We are interested in this dependence. It is worth mentioning that a similar behavior is found for networks with different values of r and also for all networks with $k_{min}=2$.

In order to consider the finite-size effects, we grew networks with $N=1\times10^4$, $N=2\times10^4$, $N=4\times10^4$, and $N=8\times10^4$ for networks with $k_{min}=1$ and $k_{min}=2$. The sample averages were performed at least with 10^2 samples (small q and large N). For large q we have used up to 3×10^4 random initial conditions.

We can see from Fig. 2 that $D(q)$ and $M(q)$ have the following asymptotic power-law behaviors:

$$M(q)\sim q^{-m}, \tag{4}$$

$$D(q)\sim q^{-d}. \tag{5}$$

Moreover, we can also see in the same figure finite-size effects for large q by comparing the behavior of the smallest network $(N=1\times10^4)$ with the largest one $(N=8\times10^4)$. In order to evaluate the exponents, we eliminate the points affected by finite-size effects and coalesce all different sets.

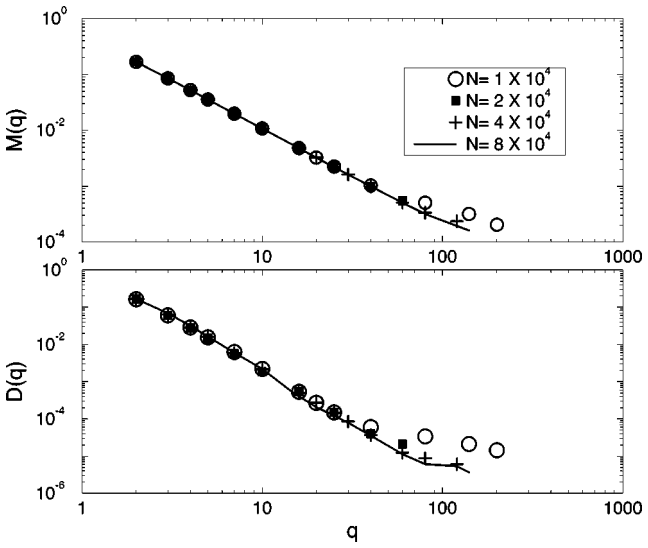

FIG. 2. Log-log plots of $M(q)$ vs q and $D(q)$ vs q for a network with $k_{min}=1$, $r=0.5$, and different N.

Finally we do a best fit. This is shown in Fig. 3 for the case defined in Fig. 2. There, the first point $(q=2)$ was not considered in the best fit. Note that we have evaluated the exponents by considering approximately 2 orders of magnitude in the q variable and that the fit is very good. In fact, in all fitted data, we obtained a correlation coefficient larger than 0.999.

Plots of $D(q)$ versus q are shown in Fig. 4 for networks with $k_{min}=1$ and different values of r [(a) $r=0.35$ and (b) $r=0.80$]. Note that the finite-size effects are present for $q\approx260$ for the $r=0.8$ and $N=8\times10^4$ case. This implies that finite-size effects appear for $q\ll k^*$, where k^* is the static cutoff. In fact, when we are evaluating the connectivity distribution $P(k)$ for this case, we expect that finite-size effects appear when $k\sim k^*=N^r\approx8\times10^3$ [26]. In a numerical simulation of the exponent γ for this case, we found that the finite-size effects appear for $k\sim1000$. Therefore, if we want

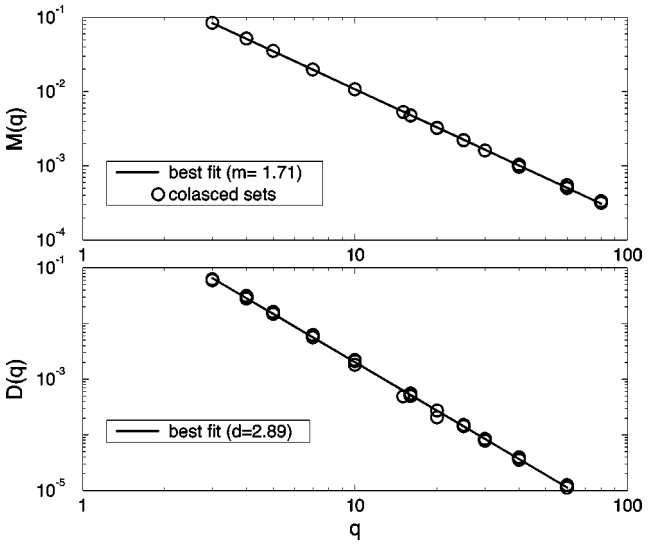

FIG. 3. Log-log plots of $M(q)$ vs q and $D(q)$ vs q for a network defined in Fig. 2. It shows the best fit of the coalesced sets.

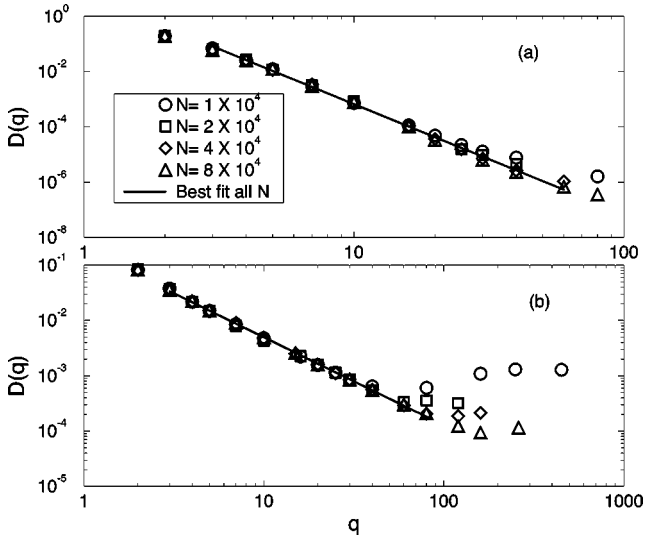

FIG. 4. Log-log plots of $D(q)$ vs q for a network with $k_{min}=1$ and (a) $r=0.35$ and (b) $r=0.80$. The best fits of the coalesced sets, after the elimination of the points affected by finite size and the discard of the first point, furnish (a) $d=3.98$ and (b) $d=1.59$.

to evaluate the exponents with 3 orders of magnitude, we must grow networks much larger than the ones we consider here.

We follow this procedure to calculate all the other exponents. They are displayed in Table I. The table also show the values of the scaling-free exponent evaluated numerically γ_n and the exact value $\gamma=1+r^{-1}$. In the numerically evaluation of γ_n we considered the same networks used in the dynamics with 10^5 samples. We can see that the exponents m and d change with r and k_{min}. It is worth mentioning that the asymptotic value of $D(q)$ is independent of the initial amount of damage. Only the short-time behavior depends on it. In particular, if the initial damage is larger than $D(q)$, $D(q,t)$ shows a decay to the stationary value.

In Fig. 5 we show the temporal evolution of $D(q,t)/q^{-d}$, for the network with $k_{min}=2$ and $r=0.5$. Note that after an initial transient, all the curves collapse.

IV. DISCUSSION OF RESULTS

In order to discuss the simulation results, we present a simple approximation for the evaluation of the exponents m

TABLE I. Exponents m and d for $k_{min}=1$ and $k_{min}=2$ for different values of r. It is also shown the scaling-free exponent evaluated numerically γ_n and the exact one γ.

	$k_{min}=1$		$k_{min}=2$			
r	m	d	m	d	γ_n	γ
0.35	2.25 (3)	3.98 (5)	2.77 (1)	4.10 (2)	3.50	3.86
0.5	1.71 (1)	2.89 (2)	2.00 (1)	2.80 (3)	2.92	3.00
0.65	1.38 (2)	2.15 (5)	-	-	2.52	2.54
0.8	1.16 (3)	1.59 (1)	0.53 (1)	0.70 (1)	2.27	2.25

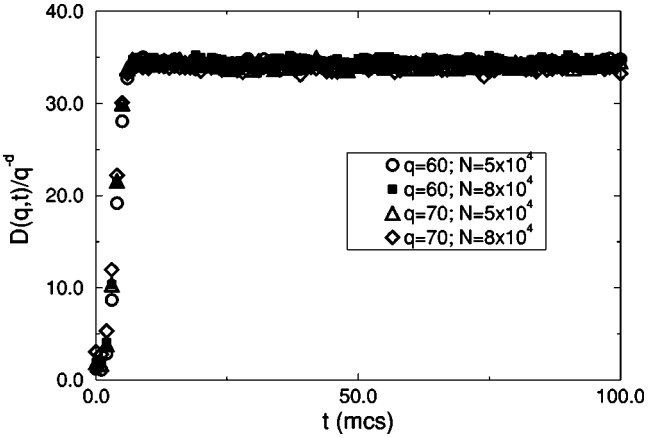

FIG. 5. Temporal evolution of $D(q,t)$ for different q and N, where $k_{min}=2$ and $r=0.5$ (see legend). The y axis was rescaled by $D(q,t)/q^{-d}$ in order to show the collapse.

and d for the case $k_{min}=1$, in which we neglect all the correlations between nodes. Note that argument is also valid for $k_{min}=2$. The dynamics defines two sublattices of nodes depending on the connectivity k of each node. The sublattices a and b consist of all nodes with $k<q$ and $k\geqslant q$, respectively. Then the nodes of sublattice $a(b)$ evolve by AND (XOR) operations. We are interested in the steady state, where the distribution of connectivity is described by $P(k)\sim k^{-\gamma}$. In this regime, we consider that a typical node i of the sublattice a with connectivity k has $\sigma_i=0$, because the AND operation of the nodes σ_i, $\sigma_1,\ldots,\sigma_k$ is 0 if at least one of these $k+1$ nodes is zero. On the other hand, a node of the sublattice b has a probability $1/2$ of being nonzero, because half of all possible configurations of σ_i, $\sigma_1,\ldots,\sigma_k$, under the XOR operation, give $\sigma_i=1$. The average density can be written in terms of the sublattices as $M(q)=M_a(q)+M_b(q)$. Since $M_a(q)\approx 0$, we have

$$M(q)\approx M_b(q)=\frac{1}{2}\int_q^\infty P(k)dk\sim q^{-(\gamma-1)}, \tag{6}$$

implying that $m=\gamma-1$. To evaluate $D(q)$ we must consider a lattice and its copy, which have evolved from two different initial states. Again we have that $D(q)=D_a(q)+D_b(q)$, where $D_j(q)$ is the contribution of the sublattice $j(j=a,b)$. So we need the number of nodes that have different values in the lattice and its copy for each one of the sublattices. Since the nodes of the sublattice a have the value 0 in both lattices, $D_a(q)\approx 0$. Only the nodes of the sublattice b can be different from 0. The probability that the same node be 1 at one lattice and 0 in its copy is $1/4$, if we neglect all correlations. Therefore we can write that

$$D(q)\approx D_b(q)\approx\frac{1}{2}\int_q^\infty P(k)dk\sim q^{-(\gamma-1)}. \tag{7}$$

Using the definition of the exponent d, we find that $d=m=\gamma-1$. From Table I, we see that the values of the exponents are different from the ones predicted by our approximated evaluation. This suggests that correlations are important in

TABLE II. Sublattice percent of $M_a(q)$ and $D_a(q)$ for $q=5$, 10, and 16 with $k_{min}=1$, $N=10^4$, and different values of r.

	M_a			D_a		
q/r	0.35	0.5	0.8	0.35	0.5	0.8
5	7%	6%	4%	0.03%	0.03%	0.01%
10	18%	16%	9%	1%	0.3%	0.01%
16	25%	24%	15%	4%	1.3%	0.3%

this problem. To obtain a better understanding we studied the steady-state behavior of the sublattices for networks with $N=10^4$ nodes. The results of the sublattice a are shown in Table II in percentages of the quantities characterizing the complete network.

Let us first analyze the case with $k_{min}=1$. From Table II, we note that the sublattice a is irrelevant for the Hamming distance independently of the value of r.

On the other hand, the contribution of this sublattice for the average density is relevant. This contribution for $r=0.35$ is larger than the one for $r=0.8$. This indicates that the sublattice a is almost irrelevant for $r=1$. To get a deep insight we analyzed $M_b(q,k)$ and $D_b(q,k)$, respectively, the average density and the average Hamming distance of nodes with connectivity k for a fixed parameter q. Note that both definitions involve only the nodes of sublattice b. From the numerical simulations we obtain that the behavior of these quantities can be described by

$$M_b(q,k) \sim A_q k^{-\alpha}, \tag{8}$$

$$D_b(q,k) \sim B_q k^{-\beta}, \tag{9}$$

with α and β having values approximately equal to γ_n, the numerical estimate of γ. This implies that $\alpha=\beta=\gamma$. Therefore, the sublattice quantities can be expressed as

$$M_b(q) = \int_q^\infty M(q,k)dk \sim A_q q^{-(\alpha-1)}, \tag{10}$$

$$D_b(q) = \int_q^\infty D(q,k)dk \sim B_q q^{-(\beta-1)}. \tag{11}$$

In Fig. 6 it is shown the graph $M_b(q,k)\times k$ for $k_{min}=1$, $r=0.5$, $N=10^4$, and $q=5,10,16$. A best fit furnishes $\alpha=2.89=\gamma_n$ and an intercept A_q, both independent of q. Similar results are obtained for the other values of the parameter r. If we neglect M_a, then we can write that $M(q)\sim M_b$ and $m=\alpha-1=\gamma-1$. Then, the exponent m should have a value near $\gamma-1$. This can be verified in Table I and the difference between $\gamma-1$ and m, which is around 20% for $r=0.35$ and 7% for $r=0.8$, is due mainly to the contribution of the sublattice a. Since this contribution becomes smaller and the exponent m approaches $\gamma-1$ as $r\to 1$, we conjecture that $m=\gamma-1=1$ when $r=1$.

Figure 6 displays $D_b(q,k)\times k$. A best fit furnishes $\beta=2.89\approx\gamma_n$ independent of q and an intercept B_q that depends on q. This dependence is due to the correlation between the

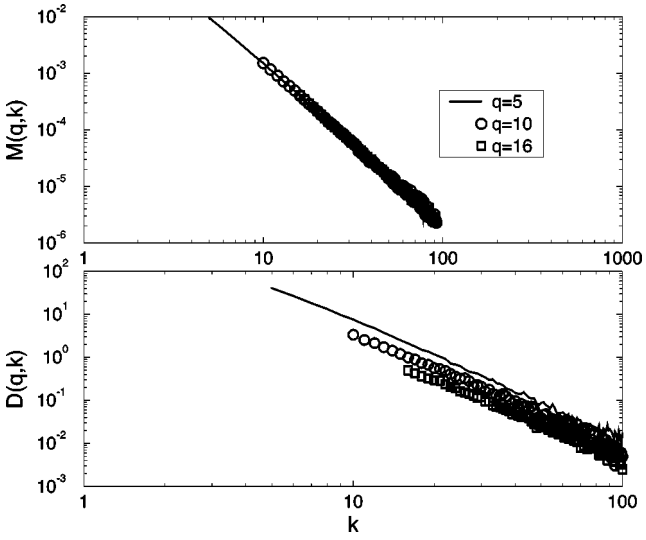

FIG. 6. Log-log plots of the sublattice b quantities $M_b(q,k)$ vs k and $D_b(q,k)$ vs k for different q, where $k_{min}=1$, $r=0.5$, and $N=10^4$.

nodes of the two sublattices. Similar results are obtained for different values of r. Since $D_a\approx 0$ independently of r, we have that $D(q)\approx D_b(q)\sim B_q q^{\beta-1}$, with $\beta-1=\gamma-1$. Then the exponent d should have a value different from $\gamma-1$ because of B_q. This is confirmed in the simulations, with the intercept presenting a power-law behavior $B_q\sim q^{-\beta_1}$. For $r=0.5$, $\beta_1\approx 1$ and we have that $d\approx\gamma$. When r becomes larger, the straight lines for different q in a log-log plot become very close, implying that $\beta_1\to 0$. Moreover, the exponent d approaches $\gamma-1$ as $r\to 1$. Then, we conjecture that $d=\gamma-1=1$ for $r=1$.

It is worth mentioning that for $r=1$, a new node is always redirected to the ancestor node. It means that we have three hubs, the initial nodes, with all other nodes connected to them. In fact we have a largest hub, with 61% of the all nodes connected to them, a smallest one (11% of connections), and a third hub with 28% of all links. During the dynamics, the XOR operation is applied to the hubs and AND to the nodes with a single link.

The exponents d and $m-0.2$ as a function of r for $k_{min}=1$ are shown in Fig. 7. Note that we included the values $m=d=1$ for $r=1$ in the data. Although we have only five points, we can do a best fit. We obtain that $d=0.963-2.836\ln(r)$ and $m-0.2=0.795r^{-0.908}$ with correlation coefficients around -0.9995.

Now, let us discuss the case $k_{min}=2$. We can see from Table III that the sublattice a is now relevant. In fact, as long as $r\to 1$, this sublattice is more important than sublattice b. Moreover, the nodes with connectivity $k=2$ are responsible for the major contribution of $D(q)$ or $M(q)$. For example, when we have that $r=0.8$ and $q=10$, they correspond to 88% of D and to 83% of M. The scenario for $r=1$ is as follows: sublattice b has no direct contribution ($D_b\approx 0$ and $M_b\approx 0$) and only the nodes with $k=k_{min}=2$ are responsible for $D(q)\neq 0$ and $M(q)\neq 0$. Now, we have three hubs, the initial nodes, with all other nodes connected to them by two links. The largest hub and the smallest one have, respectively, 52%

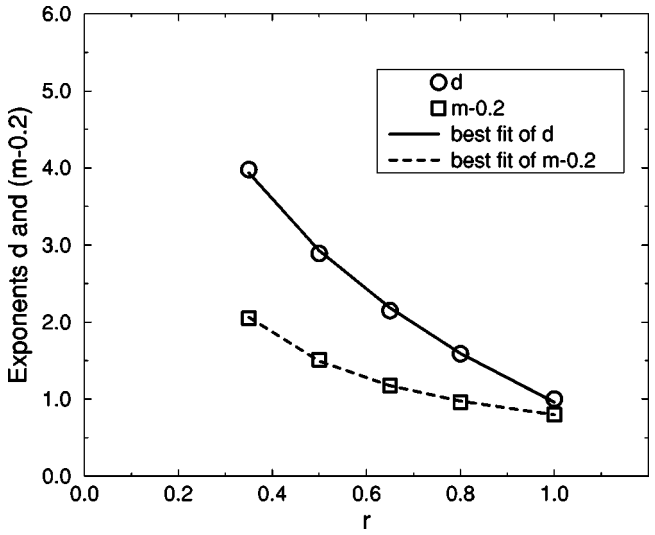

FIG. 7. Exponents d and $m-0.2$ as a function of r for $k_{min}=1$.

and 17% of the all nodes connected to them. During the dynamics, the XOR operation is applied to the hubs and AND to the other nodes. These arguments imply that the exponents d and m are not related to γ in the same way as the previous case ($k_{min}=1$).

V. SUMMARY

We have studied a deterministic Boolean dynamics with two Boolean functions (AND and XOR) controlled by an external parameter q. We have considered two distinct networks with minimum connectivity given by $k_{min}=1$ and $k_{min}=2$. In the first case, the state of a node at time $t+1$ is a function of all connected nodes plus its own value at previous time t. In the second case, the state of a node at $t+1$ depends only on the states of all connected nodes at time t. We have grown networks with different scale-free exponents by changing a parameter r. The finite-size effects were taken into account by considering networks with different sizes. We have shown that the density of the Hamming distance D and the density of 1's M as a function of q have a power-law tail for asymptotic times.

It seems that the exponents d and m characterizing the behaviors of D and M, respectively, depend on k_{min} and r; this means that the exponents depend on the details of the dynamics.

TABLE III. Sublattice percent of $M_a(q)$ and $D_a(q)$ for $q=10$ and 20 or 25 with $k_{min}=2$, $N=10^4$ and different values of r.

	M_a			D_a		
q/r	0.35	0.5	0.8	0.35	0.5	0.8
10	24%	43%	84%	32%	53%	89%
20	17%	43%	-	22%	53%	-
25	-	-	92%	-	-	95%

ACKNOWLEDGMENTS

A.C.S. thanks the hospitality of the Departamento de Fisica da Universidade de Aveiro, where part of the work took place. We thank G. J. M. Garcia for a critical reading of the manuscript. J.F.F.M. was partially supported by Project No. POCTI/FAT/46241/2002 and POCTI/MAT/46176/2002. J.K.L.S. thanks Fundação de Amparo à Pesquisa do Estado de Minas Gerais (FAPEMIG) and Conselho Nacional de Pesquisa (CNPq), Brazilian agencies.

[1] S. Kauffman, J. Theor. Biol. **22**, 437 (1969).
[2] S. Kauffman, *At Home in the Universe* (Oxford University Press, New York, 1995).
[3] A-L. Barabási and R. Albert, Science **286**, 509 (1999).
[4] A-L. Barabási, R. Albert, and H. Jeong, Physica A **272**, 173 (1999).
[5] C. Gershenson, J. Broekaert, and D. Aerts, in *Advances in Artificial Life*, edited by W. Banzhaf, J. Ziegler, and T. Christaller, Lectures Notes in Computer Science Vol. 2801 (Springer-Verlag, Heidelberg, 2003), p. 615.
[6] A. Bhattacharjya and S. Liang, Phys. Rev. Lett. **77**, 1644 (1996).
[7] I. Shmulevich, E. R. Dougherty, and W. Zhang, Proc. IEEE **90**, 1778 (2002).
[8] S. N. Coppersmith, L. P. Kadanoff, and Z. Zhang, J. Phys. D **157**, 54 (2001).
[9] S. N. Dorogovtsev and J. F. F. Mendes, *Evolution of Networks: From Biological Nets to the Internet and WWW* (Oxford University Press, Oxford, 2003).
[10] A. T. Bernardes, D. Stauffer, and J. Kertesz, Eur. Phys. J. B **25**, 123 (2002).
[11] D. J. Watts and S. H. Strogatz, Nature (London) **393**, 440 (1998).
[12] J. Lahererre and D. Sornette, Eur. Phys. J. B **2**, 525 (1998).
[13] S. Redner, Eur. Phys. J. B **4**, 131 (1998).
[14] B. A. Huberman, P. L. T. Pirolli, J. E. Pitkow, and R. J. Lukose, Science **280**, 95 (1998).
[15] R. Albert, H. Jeong, and A-L. Barabási, Nature (London) **401**, 130 (1999).
[16] B. A. Huberman and L. A. Adamic, Nature (London) **401**, 131 (1999).
[17] J. B. M. Barthélémy and L. A. N. Amaral, Phys. Rev. Lett. **82**, 3180 (1999); **82**, 5180(E) (1999).
[18] M. E. J. Newman and D. J. Watts, Phys. Lett. A **263**, 341 (1999).
[19] A. Barrat and M. Weigt, Eur. Phys. J. B **13**, 547 (2000).
[20] L. A. N. Amaral, A. Scala, M. Barthelemy, and H. E. Stanley, Proc. Natl. Acad. Sci. U.S.A. **97**, 11 149 (2000).
[21] S. N. Dorogovtsev and J. F. F. Mendes, Europhys. Lett. **50**, 1 (2000).

[22] J. J. Fox and C. C. Hill, Chaos **11**, 809 (2001).
[23] P. Uetz, Nature (London) **403**, 623 (2000).
[24] M. Aldana and P. Cluzel, Proc. Natl. Acad. Sci. U.S.A. **100**, 8713 (2003).
[25] P. L. Krapivsky and S. Redner, J. Phys. A **35**, 9517 (2002).
[26] S. N. Dorogovtsev, J. F. F. Mendes, and A. N. Samukhin, Phys. Rev. E **63**, 062101 (2001).
[27] A. Bhan, D. J. Galas, and T. G. Dewey, Bioinformatics **18**, 1486 (2002).
[28] R. W. Hamming *Coding and Information Theory* (Prentice-Hall, Englewood Cliffs, NJ, 1986).